Nuclear Engineering and Technology 49 (2017) 124–133

Available online at ScienceDirect

Nuclear Engineering and Technology

journal homepage: www.elsevier.com/locate/net

Original Article

Enhancement of Downward-Facing Saturated Boiling Heat Transfer by the Cold Spray Technique

Faruk A. Sohag [a,*], *Faith R. Beck* [a], *Lokanath Mohanta* [a], *Fan-Bill Cheung* [a], *Albert E. Segall* [b], *Timothy J. Eden* [c], *and John K. Potter* [c]

[a] *Department of Mechanical and Nuclear Engineering, Pennsylvania State University, University Park, PA 16802, USA*

[b] *Department of Engineering Science and Mechanics, Pennsylvania State University, University Park, PA 16802, USA*

[c] *Applied Research Laboratory, Pennsylvania State University, University Park, PA 16802, USA*

ARTICLE INFO

Article history:
Received 19 January 2016
Received in revised form
28 June 2016
Accepted 26 August 2016
Available online 7 September 2016

Keywords:
Cold Spray
Critical Heat Flux Limit
Downward-Facing Boiling
In-vessel Retention
Microporous Coating

ABSTRACT

In-vessel retention by passive external reactor vessel cooling under severe accident conditions is a viable approach for retention of radioactive core melt within the reactor vessel. In this study, a new and versatile coating technique known as "cold spray" that can readily be applied to operating and advanced reactors was developed to form a microporous coating on the outer surface of a simulated reactor lower head. Quenching experiments were performed under simulated in-vessel retention by passive external reactor vessel cooling conditions using test vessels with and without cold spray coatings. Quantitative measurements show that for all angular locations on the vessel outer surface, the local critical heat flux (CHF) values for the coated vessel were consistently higher than the corresponding CHF values for the bare vessel. However, it was also observed for both coated and uncoated surfaces that the local rate of boiling and local CHF limit vary appreciably along the outer surface of the test vessel. Nonetheless, results of this intriguing study clearly show that the use of cold spray coatings could enhance the local CHF limit for downward-facing boiling by > 88%.

1. Introduction

Nuclear power is known to be a clean and reliable source of energy. With proper design, nuclear power plants provide safe and consistent power under well controlled operating conditions. However, from the Three Mile Island Reactor-2 accident to the recent nuclear incident in Fukushima, Japan, it is evident that severe accidents, although highly unlikely, can occur in nuclear power plants under unexpected, extreme situations. During a severe accident, the reactor core can melt down, with molten corium relocating downward into the bottom head. In order to contain the radioactive molten corium within the reactor, it is proposed to flood the reactor cavity with water to submerge the entire reactor pressure vessel (RPV). This method, also known as in-vessel retention (IVR), allows for decay heat removal from the molten corium through the vessel wall by downward-facing boiling on the vessel outer surface. The success of IVR depends on the

* *Corresponding author.*
E-mail address: fas153@psu.edu (F.A. Sohag).
http://dx.doi.org/10.1016/j.net.2016.08.005

critical heat flux (CHF) limit for the downward-facing boiling process. To increase the thermal margin for cooling of the reactor vessel following a severe accident, it is highly desirable to develop methods to enhance the CHF limit.

The concept of IVR by passive external reactor vessel cooling (ERVC) in a flooded cavity during severe accidents is a viable approach for retention of radioactive core melt within the reactor vessel. However, the feasibility of IVR-ERVC depends on the CHF distribution of the external bottom reactor vessel surface. Owing to the practical importance of this concept, much research has been done over the past 20 years. Theofanous and Syri [1], Theofanous et al [2], and Dinh et al [3] from the ULPU facility at the University of California, Santa Barbara, performed a full-sized simulation of downward-facing boiling on the outer surface of a hemispherical RPV using a two-dimensional copper plate with separately heated zones. From the five configurations that were built, the first three were designed for the AP600 and other two for the AP1000. Configuration I simulated downward-facing boiling on the external bottom center of the vessel covering the region $-30^\circ < \theta < 30^\circ$. Configuration II simulated a full scale reactor lower head from the bottom center up to the equator ($0^\circ < \theta < 90^\circ$), while Configuration III is similar to Configuration II, but with an added thermal insulation structure. The angular location θ is measured from the stagnation point. Although there was spatial variation of CHF with θ on the vessel, the insulation structure was found to have very little effect on the local CHF limit. Configuration IV had an integrated baffle and a total of 28 burnout experiments were performed with it. The baffle structure streamlined the flow path between the RPV surface and the insulation. Despite a sudden drop in the local CHF observed at the very top of the heated wall (90°), the baffle in Configuration IV improved the CHF from Configuration III. In order to overcome the exit phenomena found in Configuration IV, Configuration V was built with four major modifications over Configuration IV which improved the local CHF limits in the heater's upper region to 1.8 MW/m^2 and approached a value of ~2.0 MW/m^2 at 90°.

Chu et al [4] conducted a full scale, three-dimensional simulation of downward-facing boiling on the exterior surface of a RPV in the Cylindrical Boiling facility at Sandia National Laboratory. Using a torispherical reactor vessel, two types of steady-state heating experiments were carried out by heating the vessel using an array of radiant lamp panels. The bottom center was consistently at the highest temperature even though edge heat flux was higher than that at the center. The cyclic nature of the vapor dynamics and the resulting two-phase motion along the heating surface for downward-facing boiling were also visually observed.

Additional quenching experiments with a copper substrate were performed by El-Genk and Glebov [5] in saturated water using two test sections of different thicknesses. Boiling curves were derived at six locations on the bottom center region and then at a local inclination angle of 8.26° along the outer surface of the test section. The heat flux increased with increasing θ in the lower heat flux region and decreased with increasing values of θ at very high heat fluxes. Interestingly, the thickness of the copper heater had no effect on the observed CHF values. CHF occurred sequentially from the lower most to the highest positions in that order. As the thickness of the test section increased, the difference in time between subsequent CHF occurrences also increased.

Cheung et al [6–9] comprehensively investigated the downward-facing boiling and CHF phenomena on the outer surface of a hemispherical vessel. The vessel and its setup included conditions with and without surrounding insulation at the Subscale Boundary Layer Boiling (SBLB) test facility at the Pennsylvania State University. A significant spatial variation of the critical heat flux was observed with a monotonically increasing local CHF limit from the bottom center to the equator of the vessel under both saturated and subcooled boiling conditions.

Later, Dizon et al [10] investigated two different methods to enhance cooling of the APR1400 reactor vessel with insulation at the SBLB facility. The first method involved the use of an enhanced vessel-insulation structure to improve steam venting through the annular bottleneck channel between the RPV and the surrounding insulation. The second method involved the use of a microporous coating on the outer surface of the vessel to promote heat transfer during downward-facing boiling. A substantial increase in the local CHF limit was observed by both methods.

Yang et al [11–13] and Yang and Cheung [14] also investigated the viability of using microporous coatings to enhance local CHF limits under IVR-ERVC conditions by performing transient quenching and steady-state boiling experiments. The microporous coatings consisted of aluminum (Al) and copper coatings on Al and stainless steel (SS) vessels. The measured local boiling curves and CHF limits for the coated vessels showed substantial enhancement compared to the uncoated vessels. The steady-state boiling experiments also confirmed the durability of the microporous coatings after many cycles of heating and quenching.

Rainey and You [15] also investigated the effect of orientation and surface enhancement of nucleate boiling on flat surfaces made of copper. For these experiments, the surfaces were coated with diamond particles and it was demonstrated that surface orientation had no effect on the heat transfer for the coated surfaces. Furthermore, a large number of active nucleation sites, due to the coating, made the surfaces immune to variation in heater size. In a similar vein, Pranoto et al [16] studied various block and fin graphite configurations with increased nucleation sites and obtained enhanced heat transfer. Additional studies by El-Genk and Parker [17] found that porous graphite at different orientations gave rise to higher nucleate boiling heat transfer coefficients under both saturated and subcooled boiling conditions when FC-72 and HFE-7100 were used as the working fluid. A higher nucleate boiling heat transfer coefficient was observed for FC-72 compared with HFE-7100, with the values higher with increasing liquid subcooling.

More recently, Ho et al [18] investigated the effects of carbon nanotube (CNT) coated surfaces and surface orientation under saturated pool boiling conditions. Pool boiling was performed in FC-72 under atmospheric conditions for two surfaces; one surface was fully coated with CNTs and the other was patterned with an interlaced CNT coating. Both coatings were on top of a silicon substrate. A 42% increase in the average heat transfer coefficient was observed for both the coated and uncoated surfaces.

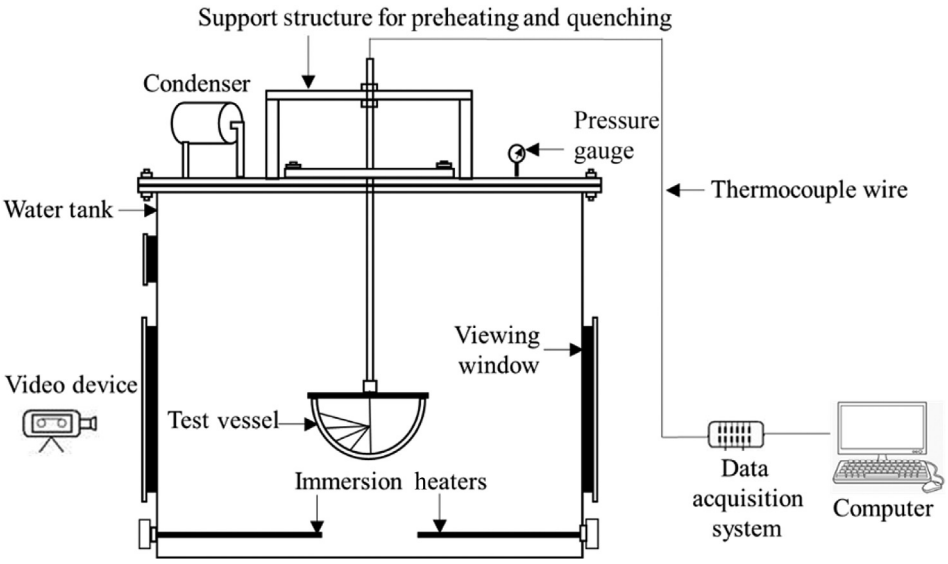

Fig. 1 – Schematic of the quenching setup in the subscale boundary layer boiling test facility.

It is now widely recognized that microporous coatings have the ability to enhance the local CHF limits for downward-facing boiling on flat and curved heating surfaces, including the RPV outer surface under IVR-ERVC conditions. However, the existing coating techniques require heat treatment on the vessel wall, which is not feasible for commercial-size nuclear reactors due to the large thermal mass involved. Moreover, it is not feasible to cure the coatings on the vessel outer surface at elevated temperatures. Furthermore, due to the requirements of specialized equipment and facilities, existing thermal coating techniques are not amenable to large reactor vessels currently in operation and/or under construction. In this study, a new and versatile coating technique known as "cold spray" that does not require heat treatment and could be used at existing and/or new sites was developed to form a microporous coating on a hemispherical test vessel made of SS. Quenching experiments were performed under simulated IVR-ERVC conditions using the cold spray coated vessel to determine quantitatively the amount of downward-facing boiling heat transfer enhancement over the corresponding case without coating.

2. Experimental method

2.1. *Experimental facility (SBLB)*

Quenching experiments were carried out in the SBLB test facility at Pennsylvania State University to simulate downward-facing boiling phenomena on the outer surface of a scaled model of RPV. The test facility, shown schematically in Fig. 1, consists of a water tank, condenser, preheating and plunging support structures, a data acquisition system, photographic system, hemispherical test vessels with and without cold spray coatings, and a heating mantle for spatially uniform heating of the vessels. The water tank is cylindrical in shape, 1.14 m tall and 1.22 m in diameter. The setup simulates the reactor cavity of a nuclear power plant that is sufficiently large to minimize recirculation motions generated due to boiling. The water tank is made of carbon steel. Three internal thermocouples located near the bottom, middle, and top of the tank monitor the temperature variation. Two large acrylic viewing windows are located on either side of the tank for visualization of the boiling process on the vessel outer surface. A condenser assembly is incorporated into the test facility, which allows for the study of pressure effects on the critical heat flux while maintaining the water level within the tank. The SBLB facility has been operated under steady-state boiling as well as transient quenching conditions. For the focus of this paper, the condenser assembly was only used to maintain the water level in the tank.

A support structure was built for preheating and quenching the test vessel. Should the vessel be plunged at any angle other than the vertical, buoyancy forces along the vessel outer surface would present an additional unwanted angular effect on the data; to maintain a vertical orientation of the test vessel during quenching, the top cover of the vessel is attached to a hollow SS rod that slides through the support structure and is guided by a bearing fixed to the top of the Al flat plate by bolts. Two adjustable stoppers fixed along the sliding rod ensure the desired preheating location of the test vessels and their plunging depth in the tank. To achieve a uniform temperature throughout the test vessels, a customized heating mantle that allows well-controlled uniform heating of the test vessels was designed and fabricated. The mantle has additional features such as easy to fabricate, hassle-free replacement of broken components with minimum cost, and reasonable amount of time required for in-house fabrication, and is shown schematically in Fig. 2.

2.2. *Preparation of test vessels*

The bare and cold spray-coated hemispherical vessels were premade from 304 grade SS. The test vessels have an outside diameter of 0.305 m with a 2.54 mm wall thickness. SS was the

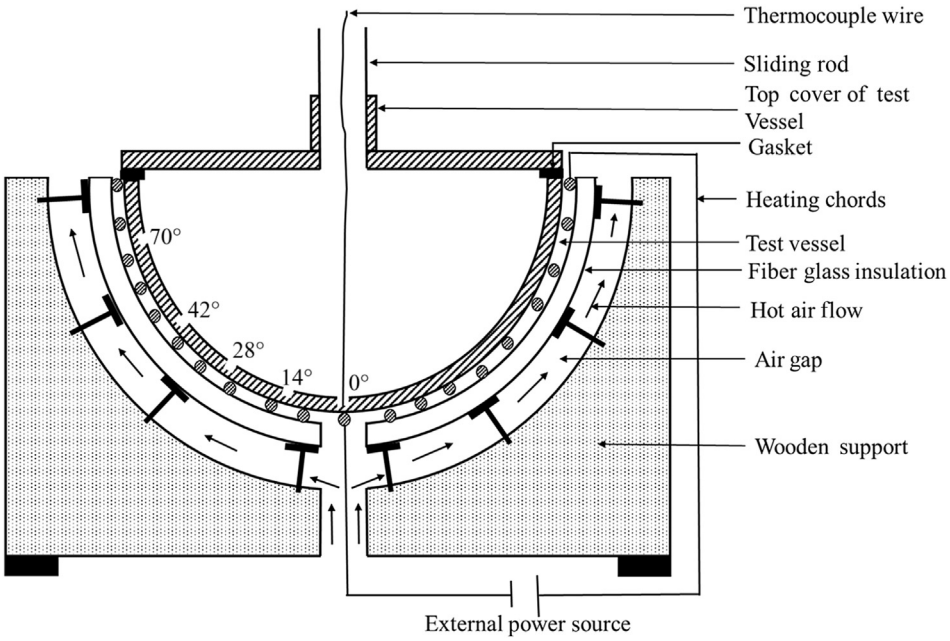

Fig. 2 – Schematic of the test vessel being preheated by the customized heating mantle.

desired material to use because it is corrosion resistant, durable, low cost, and comparable to the material used in commercial reactor lower heads. The vessel head was sealed with a top cover and an O-ring to prevent leakage and was attached to the lid by a welded flange that was connected by bolts.

In order to attach the top cover to the vessel, a same grade SS flange was welded to the test vessel. The flange has a slot for the O-ring to prevent leakage and 14 bolts to ensure leak tightness. A total of five 36-gauge k-type insulated thermocouples were spot welded along an arc starting from bottom center up to near the equator of the vessel. Holes of 3.81 mm width and depth of 1.905 mm were drilled in the inner surface along prescribed angular locations for mounting the thermocouples. The thermocouples were spot welded as close as possible to the center of the drilled holes. Finally, the thermocouples were fed through the hollow SS rod and then connected to the data acquisition system for data collection. Fig. 2 shows a schematic of a test vessel mounted on the customized heating mantle.

2.3. *Cold spray technique*

To enhance boiling heat transfer, the test vessel was coated with a microporous coating using the extremely versatile cold spray technique [19–21]. Cold spray is a very promising low-temperature direct-spray method that rapidly and efficiently creates or repairs coatings by exposing the substrate to a high-velocity jet with solid particles. In this technique, metal powders of size 5–45 μm are injected into a jet of compressed and heated nitrogen gas. A converging–diverging nozzle is used to expand the gas to supersonic conditions.

Typical gas temperature and pressures are maintained in the range 23–1,000°C and 1.5–7.5 MPa, respectively. When the gas expands, the particles present in the jet are accelerated to velocities ranging from 450–1,200 m/s. Upon exiting the nozzle, the high velocity particles impact the substrate located approximately 5–25 mm away from the exit of the nozzle. During impact, the ductile particles undergo plastic deformation at high strain rates, creating a mechanical bond between dissimilar metals or a mechanical/metallurgical bond in similar metals. A schematic of the cold spray system is shown in Fig. 3. This process is economical, environmentally friendly, and easy to implement in flexible and portable systems. In particular, it can readily be applied to operating and advanced reactors.

The microporous coating was formed on the test vessel by depositing a mixture of SS and Al as the sacrificial element. To ensure the desired coating porosity (including interconnectivity), a chemical etching with NaOH solution after deposition was used to remove the sacrificial Al particles. A weight ratio of 90% SS and 10% Al was chosen for coating the vessel. The porous layer thickness was approximately 200 μm with a relatively uniform porosity of 15% throughout the entire vessel. The representative pore size is approximately 25 μm. Fig. 4 shows a coated test vessel and an image by optical microscope of the coating cross-section.

2.4. *Experimental procedure*

Prior to quenching, the water tank was filled with filtered water and preheated to 100°C by three 12-kW immersion heaters. Heating was required between 5 h and 6 h to reach saturation. The test vessel was then installed with all five thermocouples connected to a data acquisition system. To heat the test vessel, an in-house customized heating mantle was used. Heating was performed in 5-minute intervals to promote heat diffusion and temperature uniformity in the vessel. Heating was continued until the vessel temperature reached ~350°C which is appreciably higher than the minimum film boiling temperature. The temperatures of both the

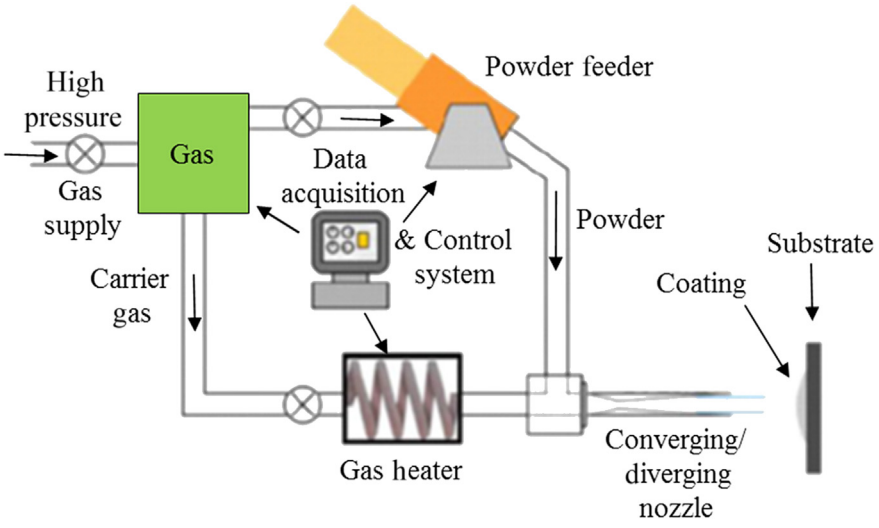

Fig. 3 – Schematic of the cold spray system.

water tank and the test vessel were monitored using the LabVIEW program. Once the test vessel reached the desired temperature, it was quenched in the water tank. Typical sliding speed of ~1 m/s was maintained and took approximately 0.3 s to completely submerge the test vessels. All data were then recorded by both the data acquisition system and visually by a high resolution camera. To verify the reproducibility of the data, a selected number of runs were repeated under identical test conditions. Following the procedure described by Yang et al. [12], the uncertainty in the thermocouple locations was ± 0.001 m. Additionally, the estimated uncertainty in temperature measurement was found to be ± 0.3°C while the maximum error in heat flux measurement above 0.1 MW/m^2 was ± 7%.

3. Numerical data reduction technique

The thickness of the vessel is very small compared with its diameter. The temperature gradient along the inclination angle is negligible when compared with the radial (wall-thickness) temperature gradient. Because of this dominant temperature gradient in the radial direction, the use of a local one-dimensional transient heat conduction analysis is sufficient for surface temperature and wall heat flux computation. For the quenching experiments, temperatures were measured on the inner surface of the vessel. To determine the temperatures along the outer surface of the vessel and the corresponding wall heat fluxes, the following one-dimensional transient heat conduction equation was used:

$$\frac{\partial T(x,t)}{\partial t} = \alpha \frac{\partial^2 T(x,t)}{\partial x^2} \quad (1)$$

where $T(x,t)$ is the local wall temperature within the test vessel at a given angular location. The thermal diffusivity α of the test vessel depends on the thermal conductivity (k), density (ρ), and specific heat (c_p) of the vessel material. The boundary conditions are: (1) a thermally insulated interior, i.e., zero heat flux on the inner surface of the vessel, i.e., $dT/dx = 0$ at $x = 0$; and (2) the measured time variation of the inner vessel surface temperature $T(x = 0,t)$. The initial condition is simply the initial temperature before quenching, $T(x,0)$.

The fully implicit method was employed to solve Eq. (1) with the above boundary and initial conditions. Time and space were divided into N_t and N_x nodes with the step sizes of

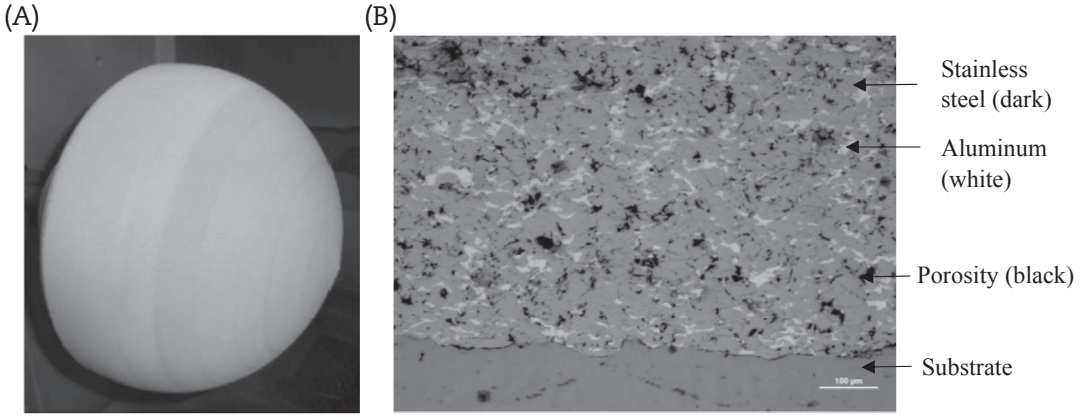

Fig. 4 – Vessels. (A) Microporous coated test vessel and (B) microscopic image of the coating at 100×.

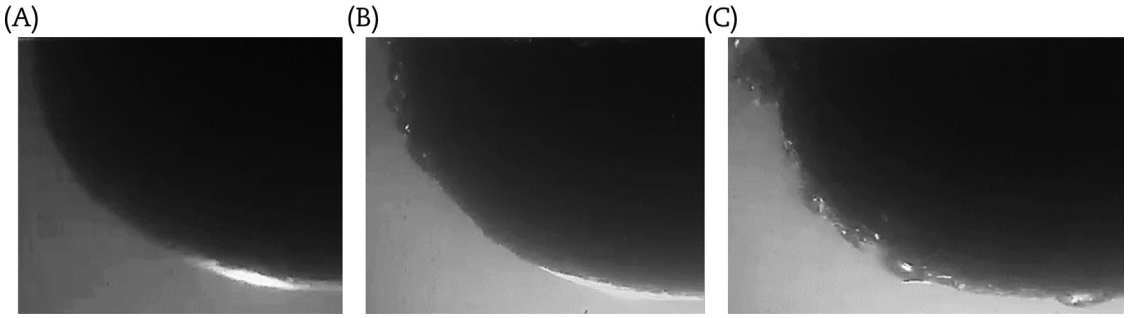

Fig. 5 – Quenching phenomena observed for the bare vessel. (A) t = 0 s; (B) t =10 s; (C) t = 20 s.

Δt and Δx, respectively. Using a first order backward differencing scheme for the time derivative and a central differencing scheme for the spatial derivatives, the following equation can be formulated:

$$\frac{T_{i,j+1} - T_{i,j}}{\Delta t} = \alpha\left[\frac{T_{i+1,j+1} - 2T_{i,j+1} + T_{i-1,j+1}}{\Delta x^2}\right] \quad (2)$$

Using the first boundary condition, Eq. (2) for i=1 and all j becomes

$$T_{i+1,j+1} = \frac{(1+2r)T_{i,j+1} - T_{i,j}}{2r} \quad (3)$$

where $r = \alpha\Delta t/\Delta x^2$.

For the rest of the nodes in space and time, Eq. (2) takes the following form:

$$T_{i+1,j+1} = \frac{(1+2r)T_{i,j+1} - rT_{i-1,j+1} - T_{i,j}}{r} \quad (4)$$

For the coated vessel, an additional interfacial condition was needed. Moreover, to improve the accuracy of the heat flux calculations, a finer step size of Δx_2 in x was used in the coated region. Considering the continuity conditions for the temperature and heat flux on both sides of the interface, the following equation was used at the interfacial nodes:

$$T_{i+1,j+1} = \frac{(1+s)T_{i,j+1} - T_{i-1,j+1}}{s} \quad (5)$$

where $s = k_c\Delta x/k_w\Delta x_2$. In the above expression, k_c and k_w are the thermal conductivities of the coating and vessel wall, respectively. Solving Eqs. (1–5), all nodal temperatures can be obtained. Once the temperatures are determined, the local outer surface heat flux can be computed using a second order backward difference equation:

$$q'' = -k\frac{3T_{N_x,j+1} - 4T_{N_x-1,j+1} + T_{N_x-2,j+1}}{2\Delta x} \quad (6)$$

where k is k_w for the bare vessel calculations and k is k_c (effective coating thermal conductivity) for the coated vessel. The effective coating thermal conductivity (k_c) was calculated from the volume fraction weighted average of the individual elements. Comparing the thermal conductivity of the bare SS vessel with that of the coated vessel, it was found that the uncertainty in the variation is small for the heat flux evaluation. Since the computed temperature and wall heat flux are first-order accurate, additional uncertainty is incurred in calculating the total uncertainty for these quantities.

4. Results and discussions

4.1. *Visualization of the quenching process*

Visualizations of the quenching processes for the bare and coated vessels, under identical conditions (i.e., same initial vessel temperature and saturated water temperature) were performed to identify the differences in the downward-facing boiling and CHF characteristics. Figs. 5 and 6 show the quenching process for the bare and coated vessels, respectively, with sequential images at three time steps. Time t = 0 refers to the instant of quenching when the vessel was completely submerged in the water tank. Based on the quantitative results and direct visualization, the following observations can be made. The coated vessel quenched in approximately 3 s, much faster than the bare vessel which required 20 s as shown in Figs. 5 and 6. A faster quench time indicates a higher cooling rate for the coated vessel than the

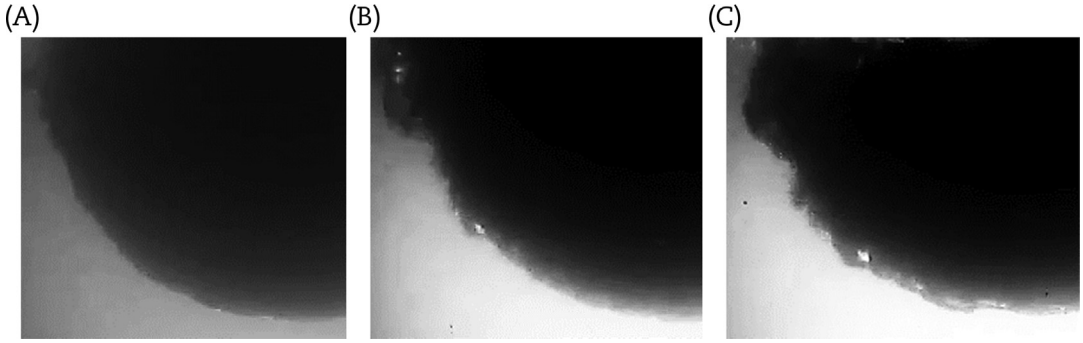

Fig. 6 – Quenching phenomena observed for the coated vessel. (A) t = 0 s; (B) t =2 s; (C) t = 3 s.

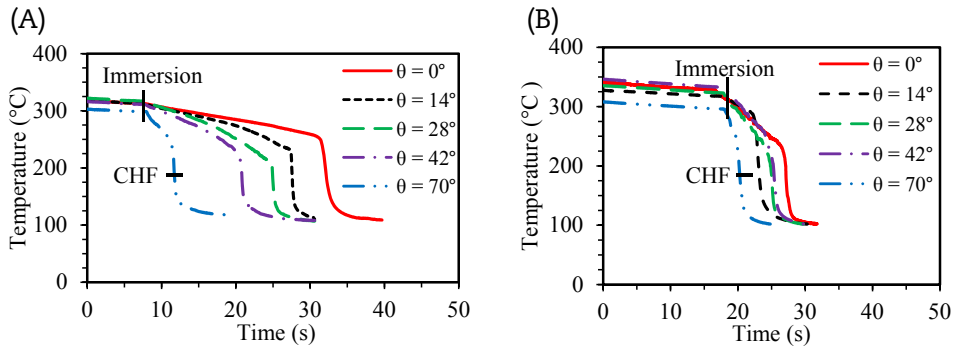

Fig. 7 – Local quenching curves observed during quenching. (A) Bare vessel and (B) coated vessel. CHF – critical heat flux.

bare vessel. A stable vapor film was observed in the initial stages of quenching for the bare vessel, indicative of film boiling heat transfer as depicted in Fig. 5A. Transition from film to nucleate boiling did not occur until more than 19 s into the boiling process, shown in Fig. 5. A wavy film was observed at the beginning of quenching for the coated vessel as seen from Fig. 6A. Transition from the film to nucleate boiling regime occurred almost within 2 s at all angular locations except the bottom center region (Fig. 6B). This quick transition indicates that the minimum film boiling temperature for the coated vessel is considerably higher than that for the bare vessel.

For both vessels, transition from film to nucleate boiling first took place at the upper angular locations on the vessels and then propagated downward toward the bottom center (Figs. 5 and 6). Although the bottom center region of the vessel was the first section to be submerged in water, it did not quench until the upper portion was completely quenched. Evidently, the local rate of boiling heat transfer (i.e., the local cooling rate) was lowest at the bottom center and it increased from the bottom center toward the upper portion of the vessel. Figs. 5C and 6C show that the nucleate boiling regime is the prevailing mode of heat transfer once the CHF was reached. The CHF was identified by a vigorous production of large vapor masses and bubbles. As the CHF limit was approached, the vapor masses generated in the bottom center region had a dominant effect on the two-phase boundary layer flow along the outer surface of the vessel. This dominant feature was qualitatively the same for both the bare and the coated vessels.

Based on the above observations, it is apparent that the boiling curve for the coated vessel had shifted higher and to the right of the corresponding boiling curve for the bare vessel, which is verified in the quantitative results section. This provides a qualitative indication that the local CHF values for the coated vessel are higher than the corresponding CHF values for the bare vessel. Significant flow-induced vibration was observed during quenching of the coated vessel. During quenching of the coated vessel, the sliding SS tube shook strongly throughout the quenching process.

Structurally, the microporous coatings are composed of randomly arranged particles, often of microscale sizes, producing pores and interconnecting channels that provide flow paths for liquid supply and vapor escape. Evaporation occurs within the microporous coating as the liquid wets the heated wall. Physically, the heat transfer enhancement in the coated vessel is attributed to four major factors that include an upsurge in the nucleation site density, an increase in the available heat transfer surface area, an enhancement of the lateral capillary-assisted liquid flow through the porous layer towards the phase-change interface, as well as the increased availability of numerous vapor escape paths provided by the interlinked pores. Because of the interconnected voids within the porous coating, the vapor escape path is no longer dictated by the critical wavelength as a result of hydrodynamic instability. The amount of enhanced heat transfer from the coating depends not only on fluid and solid properties, but also on geometrical coating parameters such as the coating thickness and pore size distribution.

4.2. *Measured temperature transients and local CHF limits*

To establish a baseline case for comparison, quenching tests were performed using an identical (bare) test vessel without a coating. Fig. 7A shows the cooling curves measured by the embedded thermocouples at five different angular positions (0°, 14°, 28°, 42°, and 70°) on the outer surface of the bare vessel. In all the quenching curves, the quenching starts at the immersion point. Although some nonuniformity in the initial temperatures between the five angular locations are observed in Fig. 7, results of the CHF are not dependent on the initial temperatures as the initial temperatures are well above the minimum film boiling temperatures. These temperature–time curves show the time evolution from film boiling to transition boiling, up to the CHF point, and then on to nucleate boiling. The location of the local CHF limit at a given angular position corresponds to the maximum slope of the cooling curve. A representative line showing the location of the CHF point for the 70° location on both of the vessels is shown in Fig. 7. Visually, the bottom center took the longest time to quench although it was physically submerged before the upper portion. The quenching time was observed to decrease with increasing angular positions.

Comparing the cooling curves for the bare and coated vessels at the same angular locations shows that the cooling curves for the coated vessel are steeper, indicating higher local CHF values for the coated vessel compared to those for the bare vessel.

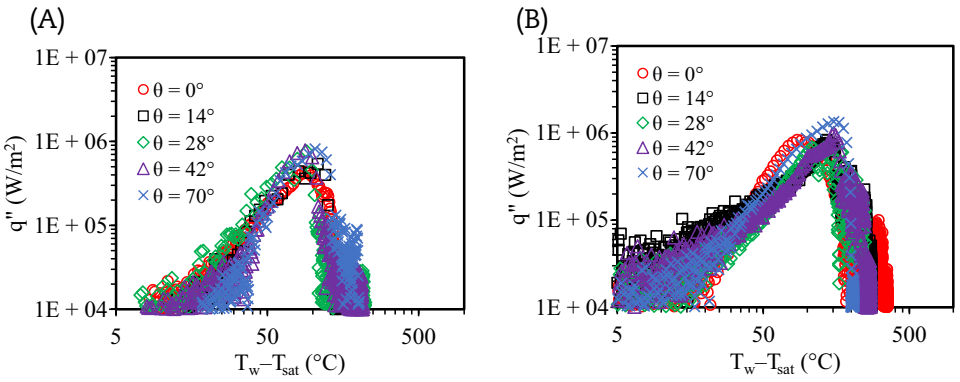

Fig. 8 – Boiling curves at different angular locations. (A) Bare; (B) coated test vessel.

Aside from differences in the cooling curves, there were also distinct variances observed in the hydrodynamic behavior (i.e., bubble dynamics) between the two vessels. During transient quenching of the coated vessel, a large vibration and noise caused by the liquid–vapor interaction occurred. For the bare vessel, this phenomenon was not observed, regardless of the initial vessel temperature; the previously described "violent" bubbling at the start of quenching was unique to the coated vessel. It was speculated that the strong capillary action at the coating-water interface was responsible for this phenomenon. The minimum film boiling temperature is higher for coated vessel which promotes early transition to nucleate boiling entailing strong capillary action in the pores. This led to the observed violent bubbling for the coated vessel.

Another observation was that even at high initial temperatures, the vapor film surrounding the coated vessel was short lived, with film boiling changing to transition boiling at a much faster rate. Typically, film boiling for the bare vessel lasted up to 19 s before transition boiling began. However, even at the same initial temperature, transient quenching for the coated vessel was characterized by a short-lived vapor film with a rapid transition to the CHF point followed by nucleate boiling. The observed behavior is understood by the boiling curves (Figs. 8 and 9) and the local CHF limits (Fig. 10).

From Fig. 8 it can be seen that for both the bare and coated vessels, the CHF increases from the bottom center to higher angular locations. Furthermore, the boiling curves shifted up and to the right for the coated vessel as compared to the bare vessel for all corresponding angular locations where the comparison is shown for the angular location of 14° only (Fig. 9). The CHF limit for the bare vessel monotonically increased with increasing angular location (Fig.10). However, for the coated vessel, the increase in CHF from the bottom center to higher locations did not follow a linear trend. As described by Yang et al [12], the bottom center of the coated vessel behaves as a singularity point where the liquid flows from all radial directions resulting in a higher local CHF enhancement. For other angular locations, the liquid supply occurs only in the longitudinal direction owing to symmetry in the circumferential direction.

For all angular positions, the local CHF for the coated vessel were 31–89% higher than the corresponding values for the bare vessel. The increase in the CHF was due to the coating structure, which improved the liquid supply to the heated surface as a consequence of the capillary effect; a suction effect occurred radially and laterally through the coating. The surface coating behaves like a thin sponge, spreading the liquid. With improved liquid supply in the phase change region, dryout occurred at a much higher wall heat flux. Since the porous coating delayed the formation of a vapor blanket by promoting nucleate boiling, the local CHF limits were enhanced.

Fig. 10 also compares the local CHF limits for the bare and coated vessels with those reported by Yang et al [11–13] and

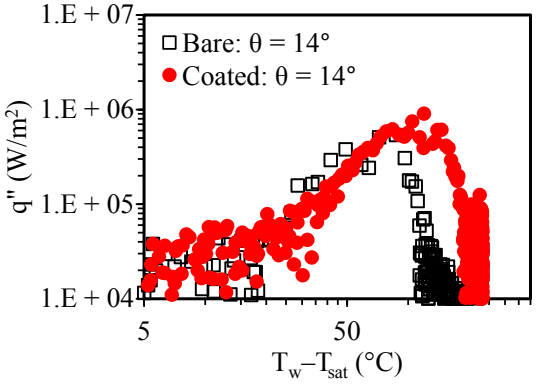

Fig. 9 – Comparison of the boiling curves between bare and coated vessels.

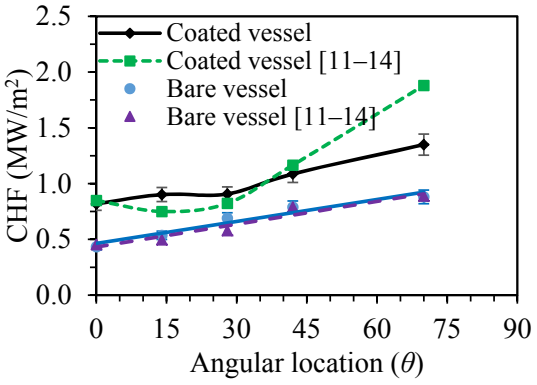

Fig. 10 – Variations of the local critical heat flux limits on the vessel outer surface. CHF – critical heat flux.

Table 1 – Comparison of the local critical heat flux (CHF) limits.

Angular location (θ)	CHF (bare) at T_w (present study) (MW/m^2 @ °C)	CHF (bare) at T_w [11–14] (MW/m^2 @ °C)	CHF (coated) at T_w (present study) (MW/m^2 @ °C)	CHF (coated) at T_w [11–14] (MW/m^2 @ °C)	% Increase in CHF with coating
0°	0.434 @ 163	0.453 @ 147	0.82 @ 187	0.849 @ 235	88.94
14°	0.537 @ 187	0.496 @ 152	0.902 @ 220	0.750 @ 192	68.15
28°	0.690 @ 170	0.578 @ 164	0.907 @ 209	0.823 @ 258	31.45
42°	0.789 @ 201	0.789 @ 163	1.087 @ 192	1.166 @ 197	37.77
70°	0.881 @ 173	0.888 @ 159	1.35 @ 196	1.880 @ 217	53.27

Yang and Cheung [14]. As can be seen from Fig. 10, the current data compared very well with that reported [11–14] for the bare vessel. It is noteworthy that Yang et al [12] experimentally observed identical CHF values for both steady-state and transient quenching experiments on a downward-facing hemispherical vessel. However, for the coated vessel at angular location of 70°, the local CHF limit was below the corresponding values reported by Yang et al using the coating formed by a heat curing method. The reason for this discrepancy is that the cold spray technique developed in this study has yet to be optimized to yield an improved microporous structure, especially at the upper portions of the test vessel.

Finally, it should be noted that the cold spray coating was found to be very durable during the testing process just described. In fact, no observable changes to the coating (spalling, debonding, degradation, etc.) were observed after many cycles of preheating, boiling, and quenching. Clearly, the results of this promising study demonstrated that the cold spray technique is indeed a viable technique for forming durable microporous coatings on commercial-size reactors that could offer an appreciable local CHF enhancement for decay heat removal under IVR-ERVC conditions. Table 1 summarizes the results from all tests, comparing the local CHF values with the temperature at which they occurred (unit in MW/m^2 at °C).

5. Summary and conclusions

A microporous coating having the composition of 90% SS and 10% Al by weight was deposited on the outer surface of a hemispherical test vessel using the cold spray technique. After deposition, the composite coating was then etched in NaOH solution to achieve a desired microporous structure with a high degree of interconnectivity. Quenching tests were performed using both bare and coated vessels to observe the downward-facing boiling process and the enhancement of the CHF from the coating. The experimental results show that the microporous coatings gave rise to greater CHF values than the bare surface. Moreover, the coatings showed a relatively high degree of robustness and fatigue resistance after exposing to multiple thermal shocks experienced during the CHF boiling tests. Based on the very promising results of this study, the following conclusions can be made:

1. The cold spray-coated vessel quenched much faster than the bare vessel under identical conditions, indicating a higher boiling heat transfer for the coated vessel.
2. For both the bare and coated vessels, transition from film to nucleate boiling first took place at the upper portion of the vessel and then propagated downward toward the bottom center. Evidently, the local rate of downward-facing boiling and the local CHF limit were appreciably higher in the upper angular positions of the vessel within the experimental conditions performed in this study. Both of these quantities were found to increase from the bottom center toward the upper portion of the vessel.
3. Quantitative results on the measured local CHF limits show that at all angular locations on the outer surface of the vessel, the local CHF values for the coated vessel are higher than the corresponding CHF values for the bare vessel given the conditions explored in this study. This clearly demonstrates that cold spray coatings could be used to enhance the thermal margin for IVR-ERVC under severe accident conditions.
4. The cold spray technique appears to be a viable technique for forming microporous coatings on substrates with different geometries and curvatures including the outer surface of a commercial-size reactor lower head.
5. Since the cold spray process and related equipment are portable, flexible, and scalable, the microporous coatings explored in this study could be utilized in new designs, as well as existing reactors provided adequate cavity space below the lower head is available.

Conflicts of interest

All authors have no conflicts of interest to declare.

Acknowledgments

This work was performed under the sponsorship of UJV Rez, Czech Republic. The authors wish to express their gratitude to Dr Jiri Zdarek of UJV Rez for his strong support and valuable technical advice.

REFERENCES

[1] T.G. Theofanous, S. Syri, The coolability limits of a reactor pressure vessel lower head, Nucl. Eng. Des. 169 (1997) 59–76.
[2] T. Theofanous, J. Tu, A. Dinh, T. Dinh, The boiling crisis phenomenon, Exp. Therm. Fluid Sci. 26 (2002) 775–792.
[3] T.N. Dinh, J.P. Tu, T. Salmassi, T.G. Theofanous, Limits of coolability in the AP1000-related ULPU-2400 configuration V facility, 10th International Topical Meeting on Nuclear Reactor Thermalhydraulics (NURETH-10), Seoul, Korea, paper G00407, 2003.

[4] T.Y. Chu, B.L. Bainbridge, R.B. Simpson, J.H. Bentz, Ex-vessel boiling experiments: laboratory- and reactor-scale testing of the flooded cavity concept for in-vessel core retention Part I: observation of quenching of downward-facing surfaces, Nucl. Eng. Des. 169 (1997) 77–88.
[5] M.S. El-Genk, A.G. Glebov, Transient pool boiling from downward-facing curved surfaces, Int. J. Heat Mass Transf. 38 (1995) 2209–2224.
[6] F.B. Cheung, K.H. Haddad, Y.C. Liu, Critical Heat Flux (CHF) Phenomenon on a Downward Facing Curved Surface: Effects of Thermal Insulation, NUREG/CR-5534, 1997.
[7] F.B. Cheung, K.H. Haddad, A hydrodynamic critical heat flux model for saturated pool boiling on a downward facing curved heating surface, Int. J. Heat Mass Transf. 40 (1997) 1291–1302.
[8] F.B. Cheung, J. Yang, M.B. Dizon, J.L. Rempe, K.Y. Suh, S.B. Kim, Scaling of downward facing boiling and steam venting in a reactor vessel/insulation system, Heat Transf. 2 (2003) 393–401.
[9] F.B. Cheung, J. Yang, M.B. Dizon, J.L. Rempe, K.Y. Suh, S.B. Kim, On the enhancement of external reactor vessel cooling of high-power reactors, 10th International Topical Meeting on Nuclear Reactor Thermalhydraulics (NURETH -10), Seoul, Korea, paper G00403, 2003.
[10] M.B. Dizon, J. Yang, F.B. Cheung, J.L. Rempe, K.Y. Suh, S.B. Kim, Effects of surface coating on nucleate boiling heat transfer from a downward facing surface, Heat Transf. 2 (2003) 403–411.
[11] J. Yang, M.B. Dizon, F.B. Cheung, J.L. Rempe, K.Y. Suh, S.B. Kim, Critical heat flux for downward facing boiling on a coated hemispherical surface, Exp. Heat Transf. 18 (2005) 223–242.
[12] J. Yang, M.B. Dizon, F.B. Cheung, J.L. Rempe, K.Y. Suh, S.B. Kim, CHF enhancement by vessel coating for external reactor vessel cooling, Nucl. Eng. Des. 236 (2006) 1089–1098.
[13] J. Yang, F.B. Cheung, J.L. Rempe, K.Y. Suh, S.B. Kim, Critical heat flux for downard-facing boiling on a coated hemispherical vessel surrounded by an insulation structure, Nucl. Eng. Technol. 38 (2006) 139–146.
[14] J. Yang, F.B. Cheung, A hydrodynamic CHF model for downward facing boiling on a coated vessel, Int. J. Heat Fluid Flow 26 (2005) 474–484.
[15] K.N. Rainey, S.M. You, Effects of heater size and orientation on pool boiling heat transfer from microporous coated surfaces, Int. J. Heat Mass Transf. 44 (2001) 2589–2599.
[16] I. Pranoto, K.C. Leong, L.W. Jin, The role of graphite foam pore structure on saturated pool boiling enhancement, Appl. Therm. Eng. 42 (2012) 163–172.
[17] M.S. El-Genk, J.L. Parker, Nucleate boiling of FC-72 and HFE-7100 on porous graphite at different orientations and liquid subcooling, Energy Convers. Manag. 49 (2008) 733–750.
[18] J.Y. Ho, K.C. Leong, C. Yang, Saturated pool boiling from carbon nanotube coated surfaces at different orientations, Int. J. Heat Mass Transf. 79 (2014) 893–904.
[19] A. Papyrin, N. Bolotina, A. Alkhimov, New Materials and Technologies, Nauka, Novosibirsk, Russia, 1992, pp. 146–168.
[20] A.E. Segall, A. Papyrin, J. Conway, D. Shapiro, A cold gas spray coating process for enhancing titanium, Proceedings of the Symposium on Innovations in Titanium Held at the 127th TMS Annual Meeting, San Antonio, TX, 1998. pp. 52–54.
[21] L. Stark, I. Smid, A.E. Segall, T. Eden, J. Potter, Self-lubricating cold sprayed coatings utilizing micro-scale nickel encapsulated, hexagonal-boron-nitride, Tribol. Trans. 55 (2012) 624–630.